Effects of magnetic susceptibility artifacts and motion in evaluating the cervical neural foramina on 3DFT gradient-echo MR imaging.

J S Tsuruda and K Remley

AJNR Am J Neuroradiol 1991, 12 (2) 237-241
http://www.ajnr.org/content/12/2/237

Effects of Magnetic Susceptibility Artifacts and Motion in Evaluating the Cervical Neural Foramina on 3DFT Gradient-Echo MR Imaging

Jay S. Tsuruda[1]
Kent Remley

The purpose of this study was to evaluate in vitro the effects of magnetic susceptibility and motion on the estimation of neural foraminal diameter with three-dimensional Fourier transformation (3DFT) gradient-recalled MR imaging as compared with CT. A cervical spine phantom was constructed from desiccated human cervical vertebral bodies embedded in a water-based proteinaceous gel. The phantom was imaged with thin-section 1.5-mm axial CT and 1.5-mm axial 3DFT gradient-recalled MR using a constant TR (35 msec) and flip angle (5°), while the TE was varied from 11 to 22 msec. During imaging, the phantom either was kept stationary or underwent subtle, intermittent motion. Compared with CT, MR consistently underestimated the diameters of the neural foramina, leading to overestimation of neural foraminal stenosis. The degree of overestimation varied directly with increasing TE values, from 8% (TE = 11 msec) to 27% (TE = 22 msec). Motion artifacts also increased foraminal overestimation and mimicked osseous hypertrophy.

The effect of image degradation due to motion was noted to increase with longer TE values. Image degradation caused by magnetic susceptibility and motion artifacts can be minimized by using the shortest TE possible. We do not recommend the use of 3DFT gradient-recalled MR imaging for the evaluation of cervical radiculopathy if patient motion is anticipated.

AJNR 12:237–241, March/April 1991; *AJR* 156: May 1991

MR imaging of the cervical spine is currently the preferred method at our institution in the initial evaluation of patients with cervical radiculopathy. With the recent implementation of three-dimensional Fourier transformation (3DFT) gradient-recalled-echo (GRE) imaging for the evaluation of cervical radiculopathy [1], thin-section (1.5–2.0 mm) images that demonstrate adequate image contrast and signal-to-noise can be obtained. At our institution we have anecdotally found that in most instances 3DFT GRE images provide excellent detail of the neural foramina, comparable to that of CT images. However, in some of our patients there has been an overestimation of the degree of neural foraminal stenosis on 3DFT GRE MR when compared with CT and surgical findings. Since partial-volume effects theoretically should be reduced with thin-section 3DFT GRE imaging, a reason for this discrepancy was sought.

Magnetic susceptibility effects inherent with GRE imaging have been suggested as one possible reason for this discrepancy [2–4]. In addition, 3DFT GRE studies are also sensitive to patient motion, presumably owing to the addition of a second phase-encoded gradient, which is required for resolving the individual slices [1]. Therefore, we designed a study with a phantom model to evaluate the effects of magnetic susceptibility and/or motion on the estimation of neural foraminal diameter when using 3DFT GRE MR imaging.

Received July 17, 1990; revision requested September 24, 1990; revision received October 22, 1990; accepted October 24, 1990.

Presented at the annual meeting of the American Society of Neuroradiology, Los Angeles, March 1990.

[1] Both authors: Department of Radiology, Box 0628, University of California, San Francisco, 505 Parnassus Ave., San Francisco, CA 94143-0628. Address reprint requests to J. S. Tsuruda.

0195–6108/91/1202–0237

Materials and Methods

A phantom model was constructed with desiccated cadaveric vertebrae from the C5 through the T1 levels. The spinous processes were immobilized in clay, and a "vertebral column" was formed and embedded in a water-based proteinaceous gel. The composition of this gel [5] was specifically designed to give T1 and T2 relaxation properties that mimic soft tissue. The overall cross-sectional diameter of the entire phantom was similar to that of an adult human neck.

Thin-section CT (GE 9800 unit, General Electric, Milwaukee, WI) was performed with axial 1.5-mm-thick contiguous sections (140 kV, 120 mA, 3 sec, and 14-cm field of view [FOV]). The images were magnified two times and viewed at bone-review settings (length × width = 550 × 1500). The neural foramen was identified as the obliquely oriented soft-tissue space, immediately cephalad to the disk space, bordered by the vertebral body and uncinate process anteriorly and medially and the corresponding superior facet of the articular pillar posteriorly. A single cross-sectional diameter, representing the largest oblique cross section, was taken at each of the three levels bilaterally. All measurements were obtained by using electronic calipers while the image was visualized on the CT monitor. Since three levels were included in the phantom, a total of six foraminal measurements (two at each level) were obtained.

The identical phantom was scanned at 1.5 T (General Electric Signa unit) by using a 5-in. (12.7-cm) posterior planar surface coil. Multiple 3DFT GRE acquisitions were obtained with these parameters: 35/11,15,20,22/2 (TR/TEs/excitations), 256 × 128 × 64 matrix, 20-cm FOV, and 1.5-mm-thick partitions. The slice-select phase-encoding gradient was oriented in the z axis, thus yielding 64 axial partitions. The imaging time for this protocol was 9 min 32 sec.

The TE was varied from 11 to 22 msec for each acquisition, keeping the TR constant, and the neural foramina were electronically measured at levels identical to the locations on the CT images while viewing the images on the MR monitor with twofold magnification. Three measurements were obtained from each neural foramen and averaged. A percent difference from the CT measurement was calculated by using the formula:

$$\frac{\text{CT measurement} - \text{MR measurement}}{\text{CT measurement}} \times 100 = \%\ \text{difference}.$$

For each acquisition, the average percent difference was obtained by calculating the mean of the percent differences at all three levels.

The MR studies were then repeated using the same acquisition parameters with TE values of 11, 15, 20, or 22 msec. During the image acquisition, motion was induced by gently rocking the phantom back and forth by 2–3 mm for approximately 5 sec separated by 30 sec of nonmotion in which the phantom was returned to the same starting position. All motion was induced by hand from the same person, positioned within the bore of the magnet, for all four studies. The neural foraminal measurements were then made as before at the same levels.

Results

The average neural foraminal diameter on CT measured 5.3 mm (range, 4.8–5.8) (Fig. 1A). In all cases, the dimensions measured with MR were less; thus, overestimation of neural foraminal stenosis was a consistent finding. In the nonmotion MR studies, the sequence that correlated best with CT measurements had the shortest TE (11 msec) (Fig. 1B). In this case, the average percent difference was the smallest (8%). As the TE was increased from 11 to 22 msec, the measured foraminal diameter progressively decreased and the percent difference between the CT and MR measurements correspondingly increased up to a maximum of 27%. The results are depicted in Figure 2.

After motion was introduced during the MR acquisition, the neural foraminal measurements during motion were compared with the nonmotion sequences (Fig. 3). On the motion images, the degree of underestimation of the neural foraminal diameter (overestimation of foraminal stenosis) was uniformly greater for each selected TE (Fig. 2). The smallest amount of artifact was encountered at TE = 11 msec (17%); it increased markedly as the TE was increased. In addition, qualitative assessment from motion degradation revealed exaggerated osseous contours that mimicked osseous hypertrophy and

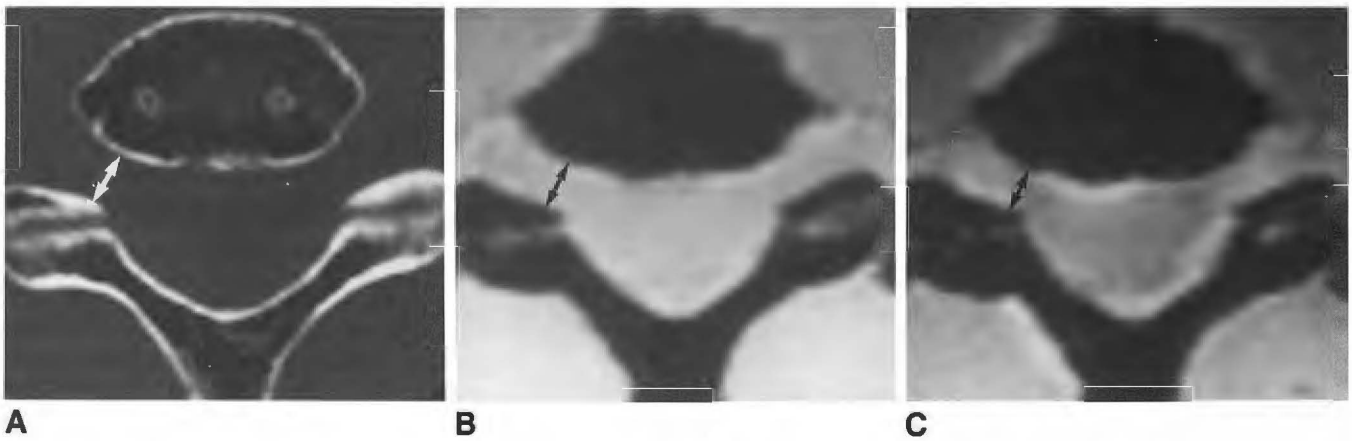

Fig. 1.—Axial sections through C7–T1 level.
***A* and *B*, CT section (*A*) and corresponding GRE 35/11 image (*B*) show similar osseous morphology of neural foramina.**
***C*, Slight irregularity and narrowing of neural foramina on GRE 35/15 image is attributed to magnetic susceptibility artifact. *Arrows* indicate typical placement of measurement cursors (see text). In this example, dimensions of right C7–T1 neural foramen were 5.3 mm (CT), 4.9 mm (GRE 35/11), and 4.4 mm (GRE 35/15).**

spur formation (Fig. 3B). In some instances, the background intensity of the soft tissue within the neural foramen and the spinal canal was quite heterogeneous, with signal loss not conforming to any anatomic structure (Fig. 3B) and approaching the intensity of bone. Accurate measurements of the neural foraminal diameter were difficult to obtain. In these cases, a gross estimate was obtained. The degree of apparent "motion" artifact was greatest with a TE of 22 msec. As a result, the data obtained at this TE were thought to be unreliable and were not included in the final results. A summary of all neural foraminal measurements is presented in Table 1.

Discussion

MR imaging of the cervical spine has proved to be a valuable tool in the evaluation of cervical radiculopathy. Previous reports have discussed the utility of spin-echo and GRE two-dimensional Fourier transformation (2DFT) imaging [2, 6] with favorable results. More recently, 3DFT GRE imaging has been reported to offer an advantage over 2DFT techniques due to the reduction of partial-volume averaging, thus improving diagnostic confidence [1].

Our clinical experience with 3DFT GRE in the routine initial evaluation of cervical radiculopathy has usually provided very good correlation with CT findings. However, on occasion, neural foraminal stenosis appears significantly greater with 3DFT GRE, producing false-positive results. Because of the variable manifestations of this apparent artifact among different patients, it was thought that magnetic susceptibility alone could not account for these findings and other factors such as patient motion may be contributory. Our phantom model was developed to investigate a possible reason for these observations.

Magnetic susceptibility artifact involving the cervical spine on 2DFT GRE imaging has been reported [3]. This artifact occurs when magnetic induction from an applied magnetic field varies between different tissues, resulting in local field inhomogeneity. Spins subjected to these intrinsic magnetic field gradients lose phase coherence, with a resulting decrease in the signal intensity of the imaging voxel. There is also spatial misregistration in areas of greatly differing magnetic susceptibility, resulting in geometric distortion with variable effect on pixel intensity [7].

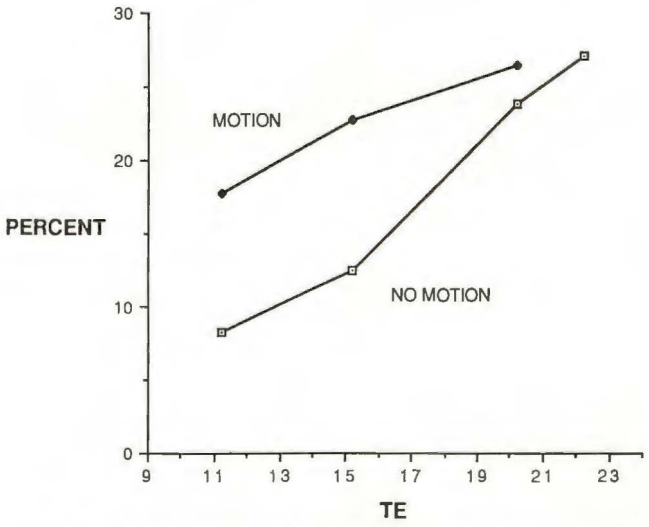

Fig. 2.—Graphic representation of percent overestimation of neural foraminal stenosis as a function of TE. Data from stationary as well as moving phantoms are shown.

TABLE 1: Foraminal Diameters at Three Different Vertebral Levels as Measured on CT and MR Images

Images Measured	Right Side/Left Side (mm)			% Difference from CT[a]
	C5–C6	C6–C7	C7–T1	
CT	5.8/5.4	5.3/5.1	5.3/4.8	–
GRE 35/11				
Without motion	5.5/5.4	4.5/4.4	4.9/4.6	8
With motion	5.0/4.4	4.4/3.8	4.3/4.4	17
GRE 35/15				
Without motion	5.4/4.8	4.4/4.3	4.4/4.6	12
With motion	5.4/4.7	4.1/3.5	3.7/3.4	22
GRE 35/20				
Without motion	5.0/4.1	4.2/3.3	4.4/3.7	23
With motion	4.9/4.0	4.5/3.1	4.3/2.9	26
GRE 35/22				
Without motion[b]	5.0/4.3	3.9/3.7	3.7/2.8	27

[a] % Difference was calculated according to the formula: [(CT measurement − MR measurement)/CT measurement] × 100.

[b] Dimensions on GRE 35/22 images obtained "with motion" were difficult to measure accurately and were not included in the final results.

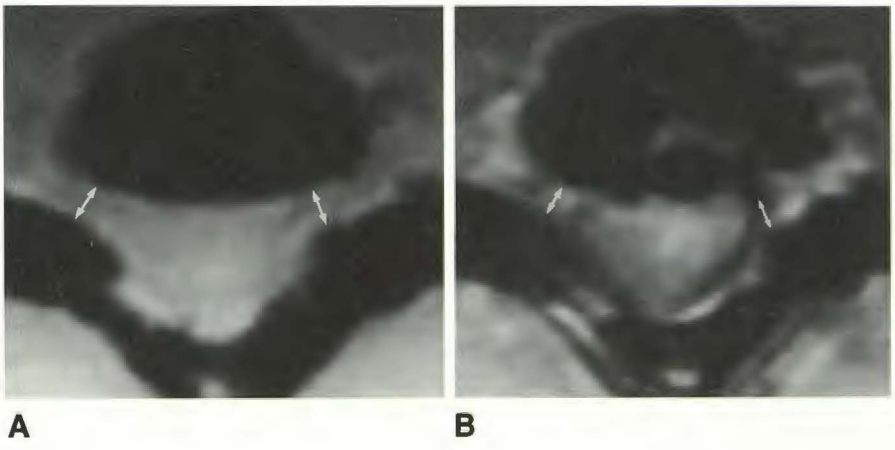

Fig. 3.—Effect of phantom motion.
***A* and *B*, GRE 35/15 images at C6–C7 level without (*A*) and with (*B*) motion. Motion-induced pseudoosseous hypertrophy resulting in overestimation of neural foraminal stenosis is evident with increased heterogeneity within soft-tissue matrix causing reduction of sharp interfaces between bone and soft tissue. In this example, left neural foramen demonstrates the greatest motion degradation and corresponding reduction in measurement accuracy (see text). Left neural foraminal dimensions are 4.3 mm without motion and approximately 3.5 mm with motion. Dimensions on right are 4.4 and 4.1 mm, respectively.**

Significant magnetic susceptibility differences have been shown to occur at bone–soft tissue interfaces such as the neural foramina, at air–soft tissue interfaces such as the skull base, or in regions of high paramagnetism such as hemorrhage [2, 4, 8]. GRE imaging is more vulnerable to this artifact than spin-echo imaging is owing to the lack of a 180° pulse; therefore, the loss of spin refocusing is sensitive to gradient inhomogeneities and the artifacts will become progressively greater as the TE or main magnetic field is increased. With increasing severity of artifacts, distortion of the bone–soft tissue interfaces on GRE images of the cervical spine results in apparent enlargement of osteophyte size and progressive narrowing of the spinal canal and neural foramina. As a result, GRE scanning should be performed with a TE of 20 msec or less [2].

In our experimental findings, the initial phantom study showed the effect of magnetic susceptibility on image quality. With a TE of 11 msec, there was reasonable correlation between MR and CT in the estimation of neural foraminal diameter (8% overestimation). However, even with a slight increase in the TE to 15 msec, there was a detectable increase in the overestimation to 12%. This degree of overestimation is important since a TE of 15 msec is the minimum possible with our current software due to the requirements of gradient-moment nulling used to reduce pulsatile CSF artifacts. As a result, the interpretation of any given clinical study needs to consider this factor. With TEs in the range of 20–22 msec, corresponding to overestimations of 23–27%, this artifact was determined to be unacceptable.

The degree of magnetic susceptibility is also directly proportional to voxel size and inversely proportional to increasing spatial resolution [9]. Larger voxels allow stronger intrinsic magnetic field gradients to build up across the imaging volume, thus causing greater geometric distortion and phase dispersion and resulting in signal loss. A constant voxel size of 1.8 mm^3 was used in this study. Although the impact of changes in voxel size was not addressed, decreasing voxel dimensions would be expected to reduce magnetic susceptibility effects in a fashion similar to TE reduction.

An attempt was made to measure the impact of hypothetical patient motion by minimally rocking the phantom in a random fashion. This motion significantly affected the accuracy of the measurements of neural foraminal diameter, with the greatest percent difference noted at the highest TE range. This was especially true when the motion-degraded study was performed with TE = 22 msec, which leads to uninterpretable images. Also, even at the shortest TE tested (TE = 11 msec), motion can still contribute to image distortion (17% vs 8% overestimation). The relative contribution of motion to image degradation was less apparent at longer TEs, that is, the two curves from Figure 2 converge. This probably occurred because the baseline (nonmotion) images at longer TEs already were degraded from magnetic susceptibility, and further motion degradation, although real, may have been somewhat obscured.

Qualitatively, phantom motion distorts the bone–soft tissue interface (Fig. 3), causing small areas of osseous hypertrophy to be enlarged and creating new regions of irregular bone contours. These findings are quite disconcerting since the amount of motion to create this artifact was quite minimal and could easily be duplicated in any given clinical setting. Also, distinguishing an abnormal finding from a motion-induced artifact is not straightforward since both may have similar morphology. Therefore, critical evaluation of fine detail is not possible if any motion degradation is being considered. The greater inhomogeneity of the background soft tissue with motion (Fig. 3A) may provide a clue to the presence of motion artifacts. However, in an actual patient study, this inhomogeneity may be less obvious owing to the greater range of soft-tissue intensities.

The genesis of the motion artifact is thought to be the additional phase-encoding gradient required to resolve individual slices or partitions in a 3DFT acquisition [1]. Therefore, motion can cause both in-plane phase-encoding artifacts as well as out-of-plane artifacts owing to movement of neighboring voxels outside the partition of interest. It should be remembered that further motion degradation in vivo may be caused by physiologic phenomena such as CSF pulsations and flow within the epidural venous plexus. Determining the exact role of these additional factors would require construction of more complex physiologic phantoms.

An additional reason for overestimation may have been the truncation artifact that is associated with the use of 128 phase-encoding steps. This type of artifact may reduce image sharpness at bone–soft tissue interfaces and can be reduced if a matrix with 256 phase-encoding steps is used. In our experimental model, a matrix with 128 phase-encoding steps was selected since this is used for our clinical patients. This smaller matrix size was selected in an attempt to reduce the total imaging time with a 3DFT acquisition [1]. The consequences of increasing the matrix size were not tested; however, it is expected that a reduction in the degree of overestimation would occur for all TE values. Nonetheless, the positive effect of reducing the truncation artifact by doubling the phase-encoding matrix (with an associated twofold increase in the imaging time to over 18 min) might be offset by the greater chance of patient motion during this longer study.

Because of our results with a phantom, we have adopted a policy of using 3DFT GRE imaging only when there is total patient cooperation. This technique is never used if even the slightest image degradation is seen on the scout sagittal localizing images. In these instances, the 3DFT acquisition should be substituted with a multislice 2DFT GRE axial sequence. Other methods of reducing motion artifacts such as improved physical restraints, psychological preparation to reduce apprehension [10], or modifying data acquisition in order to encode and compensate for motion [11, 12] need further investigation.

In summary, when imaging with short TE 3DFT GRE MR, a degree of magnetic susceptibility artifact exists that may be within acceptable limits. However, the magnetic susceptibility artifact will increase significantly when longer TEs are used. Motion artifacts cause consistent image degradation and result in both quantitative overestimation of neural foraminal stenosis and a qualitative distortion of the bone–soft tissue interface that mimics degenerative osseous hypertrophy, pos-

sibly leading to a misdiagnosis. Motion artifact also increases with longer TEs. Imaging at the shortest possible TE will reduce but not totally eliminate both magnetic susceptibility and motion artifacts. The use of 3DFT GRE MR is not recommended if patient motion is anticipated.

ACKNOWLEDGMENTS

We thank Klaus Aicher and the Contrast Media Laboratory, University of California, San Francisco, for assistance in preparation of the phantom.

REFERENCES

1. Tsuruda J, Norman D, Dillon W, Newton T, Mills D. Three-dimensional gradient-recalled MR imaging as a screening tool for the diagnosis of cervical radiculopathy. *AJNR* **1989**;10:1263–1271
2. Czervionke L, Daniels D. Cervical spine anatomy and pathologic processes. In: Lee S, Zimmerman R, eds. *The radiologic clinics of North America. Imaging in neuroradiology*, part II. Philadelphia: Saunders, **1988**:931–936
3. Czervionke L, Daniels D, Wehrli F, et al. Magnetic susceptibility artifacts in gradient-recalled echo MR imaging. *AJNR* **1988**;9:1149–1155
4. Schick R, Wismer G, Davis K. Magnetic susceptibility effects secondary to out-of-plane air in fast MR scanning. *AJNR* **1988**;9:439–442
5. Madsen E, Fullerton G. Prospective tissue-mimicking materials for use in NMR imaging phantoms. *Magn Reson Imaging* **1982**;1:135–141
6. Kulkarni M, Narayana P, McCardle C, Yeakley J, Campagna N, Wehrli F. Cervical spine MR imaging using multislice gradient echo imaging: comparison with cardiac gated spin echo. *Magn Reson Imaging* **1988**;6:517–525
7. Ludeke K, Roschmann P, Tischler R. Susceptibility artefacts in NMR imaging. *Magn Reson Imaging* **1985**;3:329–343
8. Young I, Khenia S, Thomas D, et al. Clinical magnetic susceptibility mapping of the brain. *J Comput Assist Tomogr* **1987**;11(1):2–6
9. Young I, Cox I, Bryant D, Bydder G. The benefits of increasing spatial resolution as a means of reducing artifacts due to field inhomogeneities. *Magn Reson Imaging* **1988**;6:585–590
10. Quirk M, Letendre A, Ciottone R, Lingley J. Evaluation of three psychological interventions to reduce anxiety during MR imaging. *Radiology* **1989**;173:759–762
11. Blackband S. Spatial localization for motion-rejected NMR imaging: SLOMOTION. *Magn Reson Med* **1990**;13:263–270
12. Ehman R, Felmlee J. Adaptive technique for high-definition MR imaging of moving structures. *Radiology* **1989**;173:255–263